Computational and Structural Biotechnology Journal 19 (2021) 2486–2496

COMPUTATIONAL AND STRUCTURAL BIOTECHNOLOGY JOURNAL

journal homepage: www.elsevier.com/locate/csbj

N-glycome and N-glycoproteome of a hematophagous parasitic nematode *Haemonchus*

Chunqun Wang [a], Wenjie Gao [b,c,1], Shi Yan [d,1], Xing-Quan Zhu [e], Xun Suo [f], Xin Liu [b], Nishith Gupta [a,g,h], Min Hu [a,*]

[a] *State Key Laboratory of Agricultural Microbiology, College of Veterinary Medicine, Huazhong Agricultural University, Wuhan, China*
[b] *College of Life Science and Technology, Huazhong University of Science and Technology, Wuhan, China*
[c] *College of Chemistry and Molecular Engineering, Peking University, Beijing, China*
[d] *Institut für Parasitologie, Veterinärmedizinische Universität, Wien, Austria*
[e] *State Key Laboratory of Veterinary Etiological Biology, Key Laboratory of Veterinary Parasitology of Gansu Province, Lanzhou Veterinary Research Institute, Chinese Academy of Agricultural Sciences, Lanzhou, China*
[f] *State Key Laboratory of Agrobiotechnology, China Agricultural University, Beijing, China*
[g] *Department of Molecular Parasitology, Faculty of Life Sciences, Humboldt University, Berlin, Germany*
[h] *Department of Biological Sciences, Birla Institute of Technology and Science Pilani (BITS-P), Hyderabad, India*

ARTICLE INFO

Article history:
Received 4 January 2021
Received in revised form 14 April 2021
Accepted 16 April 2021
Available online 18 April 2021

Keywords:
Haemonchus contortus
N-glycosylation
N-glycan
Mass spectrometry
Glycopeptide

ABSTRACT

N-glycosylation is a physiologically vital post-translational modification of proteins in eukaryotic organisms. Initial work on *Haemonchus contortus* – a blood-sucking nematode of ruminants with a broad geographical distribution – has shown that this parasite harbors N-glycans with exclusive chitobiose modifications. Besides, several immunogenic proteins (*e.g.*, amino- and metallo-peptidases) are known to be N-glycosylated in adult worms. However, an informative atlas of N-glycosylation in *H. contortus* is not yet available. Herein, we report 291 N-glycosylated proteins with a total of 425 modification sites in the parasite. Among them, many peptidase families (*e.g.*, peptidase C1 and M1) including potential vaccine targets were enriched. Notably, the glycan-rich conjugates are distributed primarily in the intestine and gonads of adult worms, and consequently hidden from the host's immune system. Collectively, these data provide a comprehensive atlas of N-glycosylation in a prevalent parasitic nematode while underlining its significance for infection, immunity and prevention.

1. Introduction

N-linked glycosylation is one of the most prominent post-translational modifications of proteins in eukaryotes. It plays pivotal roles in numerous biological processes, including protein folding, receptor-ligand interactions, immune response, and disease pathogenesis [1–3]. Glycans have high structural diversity, and are covalently attached to multiple asparagine residues of a single polypeptide [4,5]. Various configurations of modified sites and oligosaccharide chains underlie different physiological roles of glycoproteins. Hence, the glycosylation profiling of proteins is imperative to elucidate their biological importance in a given organism.

Examination of N-glycosylation involves three primary workflows: glycan profiling, glycosylation site mapping, and glycoprotein analysis. In recent years, the advent of high-precision mass spectrometry (MS) has facilitated large-scale studies of glycome and glycoproteome. Usually, hydrophilic interaction chromatography (HILIC) combined with liquid chromatography-tandem mass spectrometry (LC-MS/MS) and matrix-assisted laser desorption ionization-time of flight mass spectrometry (MALDI-ToF MS) are deployed to study glycoproteomics and glycomics [6,7]. These technologies have contributed significantly to our understanding of the molecular structures and biological networks of protein glycosylation in rodent and human cells [8,9]. In many invertebrate

Abbreviations: HILIC, hydrophilic interaction chromatography; MALDI-ToF MS, matrix-assisted laser desorption ionization-time of flight mass spectrometry; LC-MS/MS, liquid chromatography-tandem mass spectrometry; PNGase A/F, peptide-N-glycosidase A/F; Gal-Fuc, galactosylated fucose; Man, mannose; GlcNAc, N-acetylglucosamine; GalNAc, N-acetylgalactosamine; Fuc, fucose; Gal, galactose; Con A, concanavalin A; OST, oligosaccharyltransferase.

* Corresponding author at: College of Veterinary Medicine, Huazhong Agricultural University, No.1 Shizishan St., Wuhan, Hubei Province 430070, China.
E-mail address: mhu@mail.hzau.edu.cn (M. Hu).

[1] Equal contribution.

https://doi.org/10.1016/j.csbj.2021.04.038

organisms, however, especially the nematode parasites, the N-glycosylation remains poorly studied. *Haemonchus contortus* is one such widespread parasite of ruminant animals, which causes significant socioeconomic impact and ecological perturbation worldwide [10].

H. contortus encodes a multitude of glycoproteins, many with high immuno-regulatory activity [11]. An earlier study of glycans catalytically released by PNGase A revealed a wide range of N-glycosylations that are not commonly present in vertebrate glycans, such as galactosylated fucose (Gal-Fuc) and core α1,3-fucosylation [12]. Such distinct glycans are also present in the excretory/secretory discharge of the adult worms [13] and markedly induced protection correlated with the high level of antibody titers against the glycan epitopes in a vaccination trial [14]. In accord, when the N-glycosylation sites of the *H*11-4 antigen – an isoform of the known protective antigen group (*i.e.*, *H*11 complex) in *H. contortus* – were mutated, the recombinant protein displayed a significantly reduced affinity to antisera when compared to the wild-type antigen [15]. Hence, decoding the glycosylation profile in *H. contortus* is necessary to unravel protective immunity mechanisms and develop recombinant vaccines against the parasite. This work aimed to map the N-glycome and N-glycoproteome and provide a systematic scaffold for functional dissection of glycans and glycoproteins in *H. contortus* and related parasitic nematodes.

2. Material and methods

2.1. Biological reagents and chemicals

PNGase F and PNGase A were purchased from New England Biolabs (Ipswich, MA, USA). Fluorescein-conjugated lectins and 4′,6-diamidino-2-phenylindole (DAPI) were obtained from Vector Laboratories (Burlingame, CA, USA). The click maltose-HILIC tips were obtained from Dalian Institute of Chemical Physics (Dalian, China). Trypsin, sodium azide, phenylmethylsulphonyl fluoride (PMSF), porous graphitic carbon (PGC) cartridge, dimethyl sulfoxide (DMSO), 2,5-dihydroxybenzoic acid (DHB), trifluoroacetic acid (TFA) were procured from Sigma-Aldrich (St. Louis, MO, USA). Protease inhibitor cocktail, acetonitrile, and methanol were obtained from Merck KGaA (Darmstadt, Germany). Formic acid was purchased from Thermo Fisher Scientific (Waltham, MA, USA).

2.2. Parasite collection

All adult worms (mixed sexes) used herein were collected from goats at an abattoir in Hubei province (China) and were prepared as reported previously [16]. In brief, worms were identified, collected, and then extensively rinsed with sterile phosphate-buffered saline (PBS), followed by five additional washes in PBS containing 0.02% sodium azide. Three biological replicates were prepared and stored in liquid nitrogen until further use.

2.3. Protein extraction and glycopeptide enrichment

Proteins were extracted from each of three replicates. In brief, each 0.5 g of adult worms was immersed in 500 μL of ice-cold lysis buffer (8 M urea, 1% protease inhibitor cocktail) and then homogenized in a glass homogenizer for 20 min. The homogenates, kept on ice, were sonicated in 30 s bursts for 5 min. Samples were centrifuged at 10.000*g* for 25 min to remove the remaining debris. Finally, the supernatants were collected, and protein concentrations were detected using a BCA assay. Individual protein sample (400 μg) was reduced with 5 mM dithiothreitol at 56 °C for 35 min and then alkylated with 11 mM iodoacetamide at room temperature for 20 min in a dark room. The urea concentration of the sample was diluted to less than 1 M with 100 mM NH_4HCO_3 solution. Trypsin was added at a mass ratio of 1:50 (trypsin/protein) for the first digestion (overnight) and a ratio of 1:100 (trypsin/protein) for an additional 5 h. Finally, tryptic peptides were evaporated to dryness using a centrifugal evaporator (Eppendorf, Hamburg, Germany). Glycopeptides were collected using a HILIC enrichment method. Briefly, the dried peptides were reconstituted in 40 μL of loading buffer (80% ACN with 1% TFA) and then pipetted into a HILIC tip. After centrifugation (4000*g*, 20 min), glycopeptides were washed three times with 40 μL of loading buffer and centrifuged to remove the residual non-glycopeptides. Afterward, glycopeptides were eluted three times with 20 μL of 10% ACN. Finally, enriched glycopeptides were divided into two equal parts and respectively dried by the centrifugal evaporator.

2.4. Release, purification, and permethylation of N-glycans

N-glycan preparation workflow was based on a previous report with some modifications [17] (see Fig. 1). Briefly, an aliquot of glycopeptides was incubated with 2 μL of PNGase F in 50 μL of sodium phosphate buffer (pH 7.5) at 37 °C for 24 h. PNGase F-cleaved glycans were then desalted and purified by PGC cartridges, as described elsewhere [17,18]. Glycopeptides (remaining after PNGase F treatment) were dried and redissolved in 50 μL of sodium acetate solution (pH 6.0) for PNGase A (2 μL) digestion at 37 °C for 24 h. PNGase A-released glycans were isolated by PGC cartridges, as described above. Permethylation of glycans was performed following an established protocol [19]. In brief, native glycan pools released by PNGase F and PNGase A were dissolved in 50 μL DMSO, followed by the addition of DMSO-NaOH slurry (100 μL). Subsequently, 50 μL of methyl iodide was added, and the reaction mixture was shaken for 15 min at room temperature. The reaction was terminated by adding 500 μL of ultrapure water and 250 μL chloroform to separate liquid phases. The lower organic phase containing permethylated glycans was collected and washed 3x with ultrapure water. The two organic phases were transferred to separate vials and dried by the centrifugal evaporator.

2.5. MALDI-ToF and MALDI-ToF/ToF analysis

Spectra were obtained using the 5800 MALDI-MS instruments in the positive ionization mode (SCIEX, Concord, Canada). The dried glycan residues were reconstituted in 15 μL methanol solution. The matrix was prepared with 10 mg/mL DHB in 50% acetonitrile and 10 mM sodium acetate. 1 μL of permethylated glycan was mixed with 1 μL of freshly-prepared DHB before spotting on a MALDI-target plate and allowed to crystalize at room temperature. In total, 1000 laser shots were applied on each sample spot. MS/MS analyses were performed with air as CID gas using 2 kV collision energy. The final data were processed by DataExplorer 4.0 (SCIEX, Concord, Canada), and the selected spectra were annotated using GlycoWorkbench (2.1 build 146).

2.6. Lectin-fluorescence microscopy

The adult worms were flat-fixed in 4% paraformaldehyde and sliced for paraffin embedding. Samples for light microscopy (thickness, 4 μm) were incubated with fluorescein-labeled lectins overnight at 4 °C. The source and binding specificity of the lectins used are listed in Table 1. After three PBS washes, the lectin-treated sections were stained with DAPI (room temperature, 5 min) to visualize the cell nuclei and then washed 3x, each for 5 min. Samples were mounted with an anti-fading solution for fluorescence microscopy (Olympus, Tokyo, Japan). Image files were

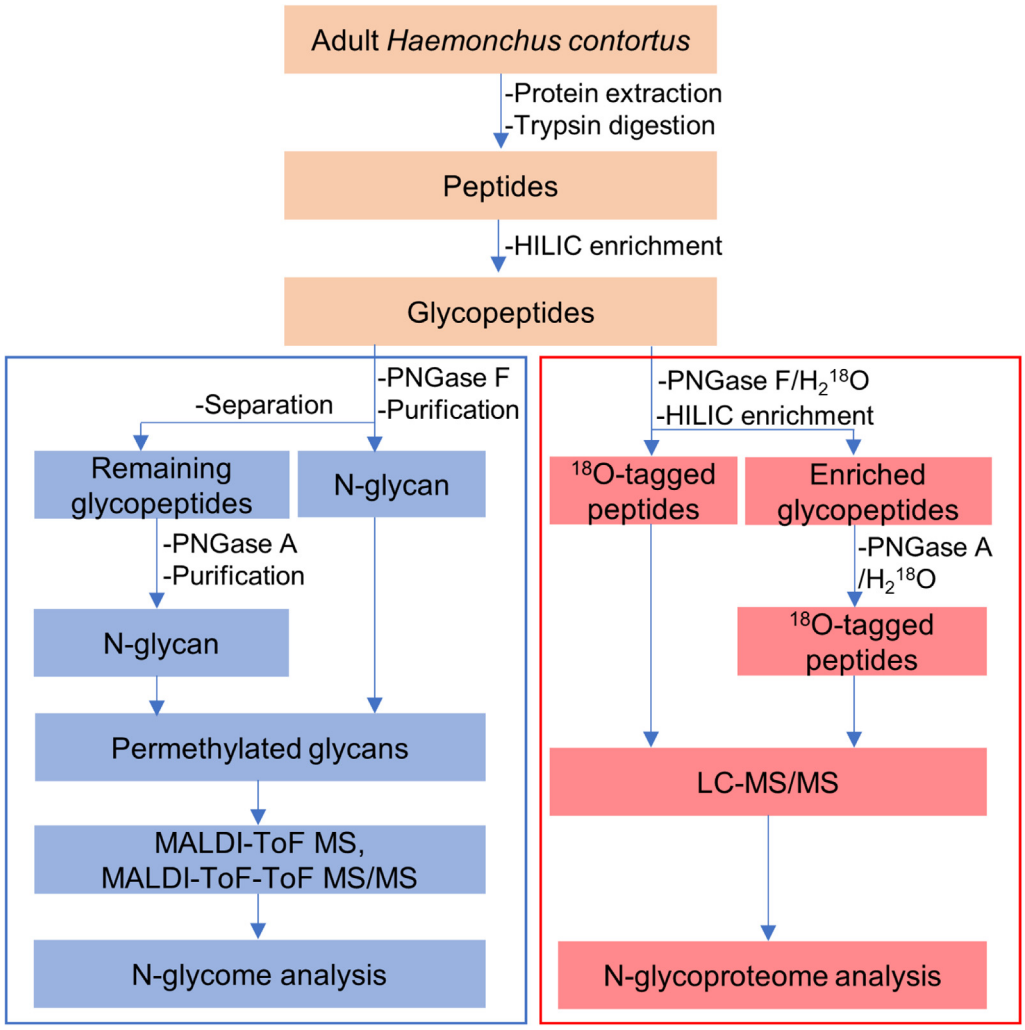

Fig. 1. Workflow of N-glycome and N-glycoproteome analysis in *Haemonchus contortus*. Trypsin-digested and HILIC-enriched glycopeptides were divided into two equal aliquots for preparing N-glycome (blue box) and N-glycoproteome (red box) samples. For N-glycome analysis, glycopeptides remaining after PNGase F treatment were further digested by PNGase A to release N-glycans with core α1,3-modified fucose. Free glycans were permethylated before MALDI-ToF MS and MS/MS analyses. For N-glycoproteome studies, glycopeptides were deglycosylated by PNGase F in heavy water. The remaining glycopeptides were further enriched by HILIC and subject to PNGase A digestion. The ^{18}O-tagged deglycosylated peptides were analyzed by LC-MS/MS. N-glycans were deduced from the recorded spectra and computational fragmentation using the GlycoWorkbench suite, whereas N-glycopeptides were identified through bioinformatic tools (see *methods*). (For interpretation of the references to color in this figure legend, the reader is referred to the web version of this article.)

Table 1
The source and binding specificity of lectins used in this study.

Abbreviation	Source	Oligosaccharide specificity	Reference
Con A	*Canavalia ensiformis*	α-linked Man, branched and terminal	[50]
WGA	*Triticum vulgaris*	Terminal GlcNAc	[51]
SBA	*Glycine max*	Terminal α, β-GalNAc	[52]
UEA-I	*Ulex europaeus*	α-Fuc	[53]

Man: Mannose; GlcNAc: N-acetylglucosamine; GalNAc: N-acetylgalactosamine; Fuc: Fucose.

scanned and analyzed using ImageJ software to semi-quantify the mean fluorescence intensity.

2.7. Deglycosylation of glycopeptides and LC-MS/MS analysis

For N-glycoproteome analysis (see Fig. 1, three replicates), deglycosylation of glycopeptides was performed by sequential digestion with PNGase F and PNGase A, as described previously [20]. Briefly, an aliquot of enriched glycopeptides was dissolved in 50 μL of 50 mM NH_4HCO_3 buffer (prepared using $H_2^{18}O$, pH 7.5), followed by deglycosylation with 2 μL PNGase F (37 °C, 24 h). As noted, the procedure was carried out in ^{18}O-water. The isotope-labeled glycosylation site-specific tagging can be distinguished from non-enzymatic deamidation [21]. The deglycosylated fraction was subjected to HILIC enrichment, as outlined above. Peptides deglycosylated by PNGase F were collected from the HILIC tip effluent. The HILIC tip-bound glycopeptides were eluted and dried by the centrifugal evaporator and finally reconstituted in 50 μL of 50 mM sodium acetate solution (in $H_2^{18}O$, pH 6.0). 2 μL of PNGase A enzyme was supplemented, followed by incubation at 37 °C for 24 h. The PNGase F- and PNGase A-deglycosylated peptides were desalted using C18 ZipTips (manufacturer's protocol), dissolved in 0.1% formic acid (solvent A), and loaded onto a reversed-phase analytical column equipped with an EASY-nLC 1000 UPLC system. A gradient at a constant flow rate of 400 nL/min was programmed to increase the solvent B (0.1% formic acid in 98% acetonitrile) from 6 to 23% in the first 26 min, followed by another 8 min from 23 to 35%, and then 3 min to reach 80%, and after that staying constant at

80% for the last 3 min. After UPLC, peptides were ionized by a nanospray ionization source (2.0 kV) and analyzed by MS/MS in Orbitrap Fusion™ Tribrid™ (Thermo Fisher Scientific, Bremen, Germany).

2.8. Database analysis

The MS/MS data were evaluated by the MaxQuant software package (v1.5.2.8). Tandem mass spectra were searched against *H. contortus* entries in the UniProt database (24277 proteins) concatenated with reverse decoy database. Trypsin was specified as the cleavage enzyme allowing up to 2 missed cleavages. The mass tolerance for precursor ions was set at 20 ppm in the first search and 5 ppm in the main search. The mass tolerance for fragment ions was set as 0.02 Dalton. Carbamidomethyl on the cysteine residue was specified as a fixed modification, and oxidation on methionine was defined as a variable modification. The false discovery rate was adjusted to $\leq$ 1%, and the minimum score for modified peptides was set at $\geq$ 40. Glycosylated sites identified herein are based on the consensus of $\geq$ 2 biological replicates.

2.9. Bioinformatic methods

The Gene Ontology Annotation (GOA) was based on the UniProt-GOA database (http://www.ebi.ac.uk/GOA/). Proteins were classified according to molecular function, cellular component, and biological process. Amino acid sequence motifs comprising at least 20 residues within +/-10 residues of the N-glycosylation sites were analyzed by the MoMo suite (http://meme-suite.org/tools/momo/). Secondary structure analysis was done using the NetSurfP program with settings as described previously [22]. The PSORTb v3.0 software package was used for predicting the subcellular location of proteins (http://www.psort.org/) [23]. The functional domains were annotated based on the InterPro database (http://www.ebi.ac.uk/interpro/) [24].

2.10. Statistics and data availability

The graphs are presented as the mean with SE from at least three independent assays unless specified otherwise. Statistical analyses were performed using GraphPad Prism software (v8.0). Significance was tested by unpaired two-tailed Student's *t*-test ($^{*}p \leq 0.05$, $^{**}p \leq 0.01$, $^{***}p \leq 0.001$). The data generated or analyzed during this work are provided in the main article and figures. The source data for the N-glycoproteomics and N-glycomics can be found in supplementary data and accessed through the PRIDE repository (PXD023379). All resources are available from the authors upon reasonable request.

3. Results

3.1. Analysis of N-glycans in Haemonchus contortus

To determine the N-glycan profile of adult worms, we digested enriched glycopeptides by PNGase F, followed by PNGase A treatment to cleave the PNGase F-resistant N-glycans with core α1,3-modified fucose residues [25]. Native N-glycans were permethylated and subsequently analyzed by MALDI-ToF MS and MS/MS. Glycan species are displayed primarily as $[M + Na]^+$ adducts on the MS spectra. The spectrum of PNGase F-released glycans (Fig. 2A) revealed the pauci-manosidic structures with or without fucose ($Hex_{2-4}HexNAc_2Fuc_{0-2}$) and high-mannose structures ($Hex_{5-9}HexNAc_2$). A significant fraction of complex-type glycans ($Hex_{3-4}HexNAc_{3-5}Fuc_{0-2}$) was also identified (Fig. 2A, Table S1). The MS data of the PNGase A-released glycans revealed an enriched pool of structures with multiple fucose residues, appearing at *m/z* 1316.0, 1346.0, 1520.1, 1694.3, and 1724.3 ($Hex_{2-4}HexNAc_2Fuc_{1-3}$, Fig. 2B and Table S1). Besides, many pauci-mannosidic and high mannose structures ($Hex_{4-9}HexNAc_2$) were detected in the PNGase A-digested pool, indicating incomplete removal of such moieties from glycopeptides by the PNGase F.

The glycan ions of selected MALDI-ToF MS spectra were further subject to MS/MS fragmentation. We observed the presence of a Gal-Fuc-like disaccharide unit on some N-glycan structures as described elsewhere [12], especially the ones possessing pauci-manosidic and truncated backbones. The representative MS/MS spectrum of a PNGase F-released glycan at *m/z* 1549.9 ($Hex_4HexNAc_2Fuc_1$, Fig. 3A) displayed three diagnostic fragment ions at *m/z* 433 (C-type ion), 678 (Y-type ion), and 894 (B-type ion), which indicated the presence of a Galβ1,4Fuc epitope linked to GlcNAc residue at the reducing end. As judged by the co-fragmentation ions (*m/z* 474, 871, 1098), the spectrum suggested the occurrence of another dominant isomer, which carries fucose on the 6-position of the proximal GlcNAc and four hexoses at the non-reducing termini. The *m/z* 433 fragments representing the Gal-Fuc-like unit appeared on the spectra of at least 7 different N-glycan moieties in both PNGase F and A released glycan pools (Table S1).

The MS/MS spectra of PNGase F-released N-glycans suggested that a significant portion carries either an LDN-like or an LDNF-like motif, as reported previously [17]. As exemplified by *m/z* of 1662.0 ($Hex_3HexNAc_4$) (Fig. 3B) and 2010.2 ($Hex_3HexNAc_4Fuc_2$) (Fig. 3C), the spectrum of the former glycan displayed diagnostic fragments at *m/z* 527 (B-type ion) and 1157 (Y-type ion), indicating a GalNAc-GlcNAc (LDN) unit. The latter glycan (*m/z* 2010.2) showed key fragments at *m/z* 701, 905, 1127, and 1332, suggesting the fucosylated LDN (LDNF) motif on its antennae. In contrast to the PNGase F, a difucosylated isomeric moiety was released by PNGase A at *m/z* 1520.1 ($Hex_3HexNAc_2Fuc_2$) (Fig. 3D). Another fragment ion at *m/z* 648 and 894 signified that the proximal GlcNAc residue is substituted at the 3- and 6-OH positions. Also, as advocated by *m/z* 433 (C-type ion) and 1109 (Z-type ion) on the same spectrum, another dominant isomer with a Gal-Fuc-like motif may exist. This isomer also carries fucose residue on the innermost reducing-end GlcNAc, as shown by the *m/z* 474 and 1068 fragments. Compared to previous findings [12,17,26], our N-glycome data mapped a much higher diversity of N-glycans in *H. contortus*, many of which contained potentially typical structures such as Gal-Fuc motifs, terminal LDN and LDNF, and core α1,3-fucosylation.

3.2. Anatomical distribution of glycosylation in Haemonchus contortus

The above data suggested the presence of pauci/high-mannose and complex N-glycans, which harbor mannose and GlcNAc/GalNAc termini, and core fucosylated structures with or without galactose capping. We, therefore, selected plant lectins with affinities to recognize these glycan moieties to discern their distribution patterns in *H. contortus* (Table 1). While differences were observed in the binding patterns (Table 2), all lectins revealed strong fluorescent intensity in the adult worms (Fig. 4). Both mannose- and GlcNAc-binding lectins (Con A and WGA) were detected in the intestine and gonad of the adult female and male worms. Con A-treated samples displayed a clear punctate signal distributed in the cytoplasm and microvilli of the intestine (Fig. 4A-B), indicating the presence of abundant α-linked mannose residues in the tissue.

Additionally, Con A stained the cement gland (the posterior segment of gonad) in males along with a relatively weaker signal in the outer cuticle (Fig. 4B-C). In contrast, WGA, which favors terminal GlcNAc, highlighted glycoconjugates located in the intestinal

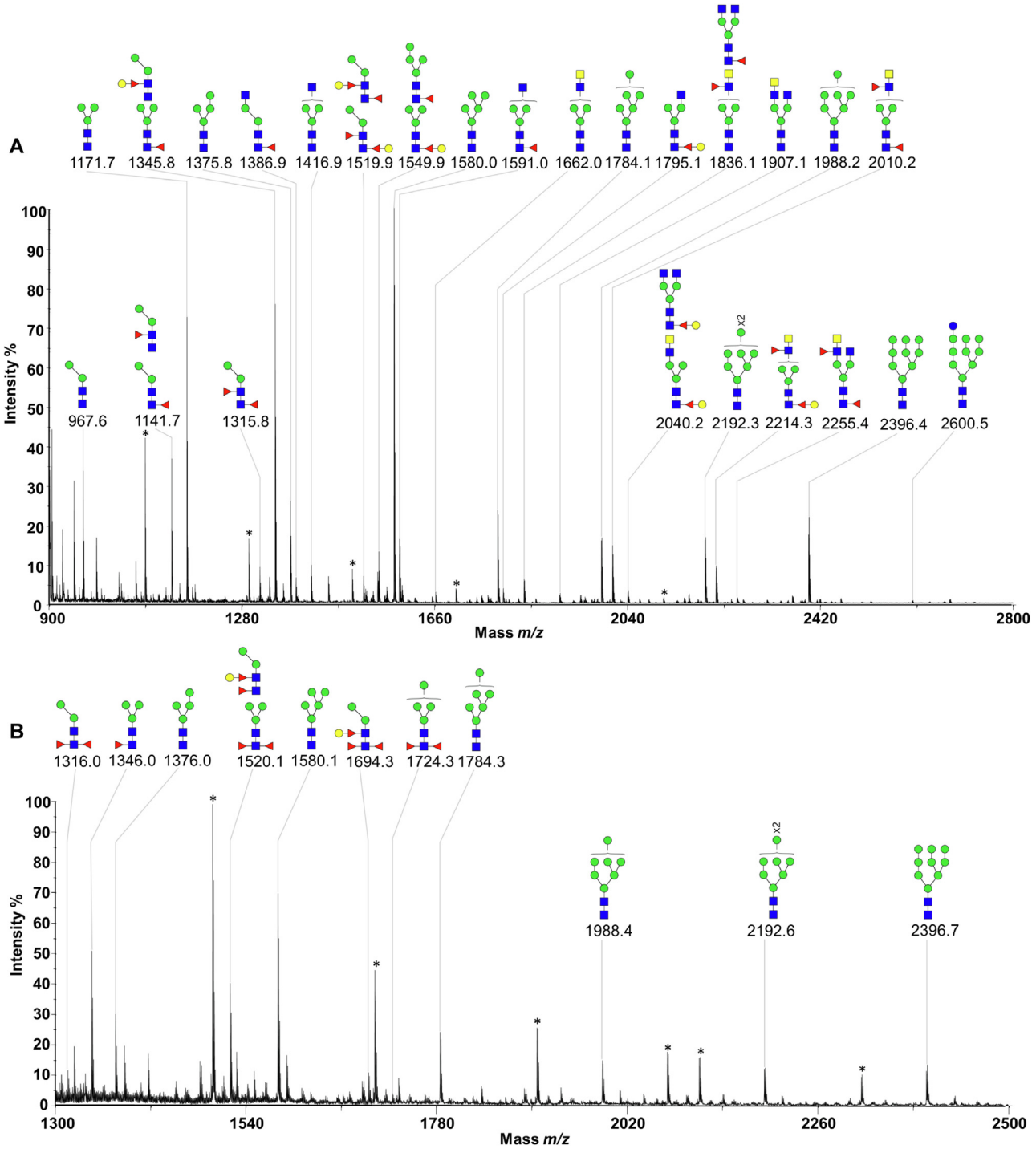

Fig. 2. MALDI-MS spectra of the permethylated N-glycans of adult *Haemonchus contortus*. N-glycans were released by digesting the worm glycopeptides with PNGase F (A), followed by PNGase A (B). Glycan species are displayed primarily as $[M + Na]^+$ adducts. Peaks are annotated using the symbol nomenclature (green circle, mannose; yellow circle, galactose; blue circle, glucose; blue square, GlcNAc; yellow square, GalNAc; red triangle, fucose). The N-glycan structures were deduced based on the MALDI-ToF MS/MS fragmentation and the current knowledge of N-glycan biosynthesis in nematodes. Co-purified hexose oligomers are marked with *asterisks*. (For interpretation of the references to color in this figure legend, the reader is referred to the web version of this article.)

microvilli of both sexes, ovaries of females, and male adults' cement gland. The latter appeared to superimpose with the distribution pattern of Con A-bound glycoconjugates.

SBA, having broad specificity to the terminal GalNAc, recognized the ovaries in female worms (Fig. 4A), which suggests the occurrence of N-glycoproteins with β-linked GalNAc termini, presumably due to the presence of the LDN and/or LDNF epitope. Notably, fucose residues were detected (by UEA-I) mainly in the intestinal cytoplasm of the female adult worms (Fig. 4A-C). Collectively, our lectin binding assays indicated an abundant expression of mannose-, terminal GlcNAc/GalNAc- and fucose-rich glycoconjugates and thereby endorsed the N-glycome analysis, as described elsewhere in this work.

3.3. Identification of N-glycoproteome and N-glycosylation sites

Next, we performed HILIC enrichment in conjunction with LC-MS/MS to identify PNGase F- and PNGase A-deglycosylated

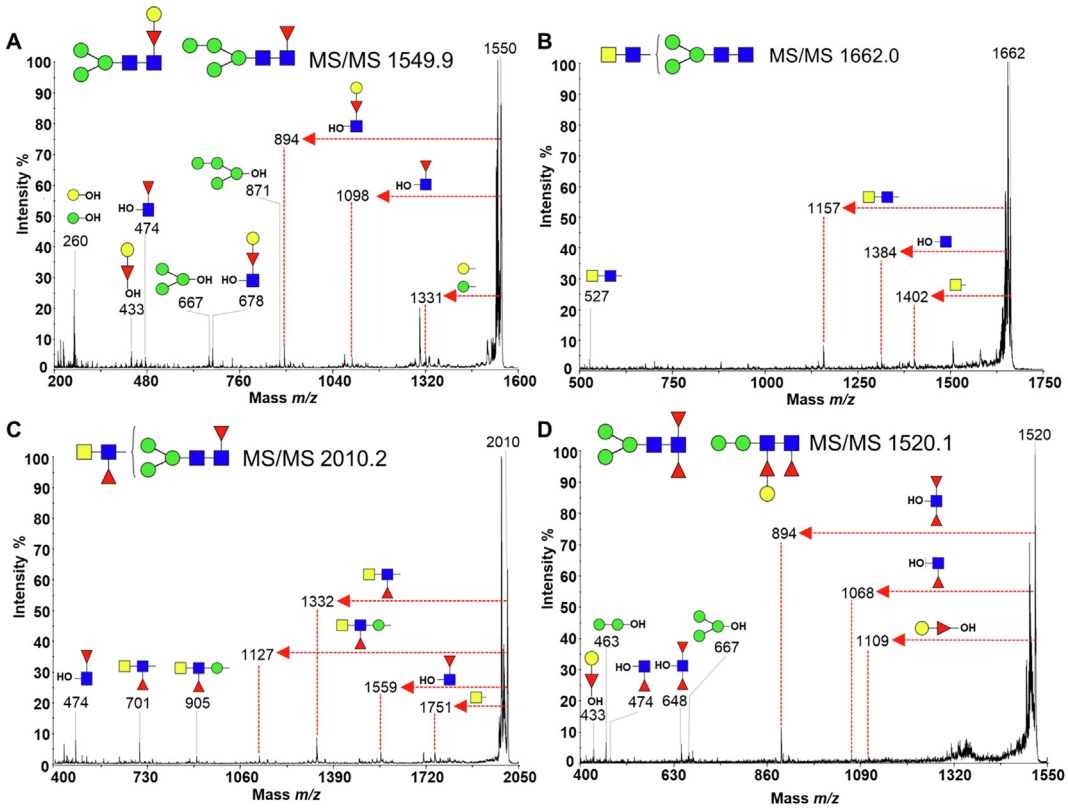

Fig. 3. MALDI-ToF MS/MS spectra of the permethylated N-glycans released by digestion of *Haemonchus contortus* glycopeptides by PNGase F (A-C) and PNGase A (D). Peaks at *m/z* 1549.9 (A), 1662.0 (B), 2010.2 (C) and 1520.1 (D) are depicted. The red dotted arrows represent the loss of indicated fragments from the glycan ion. The predicted N-glycan configuration is shown by symbol nomenclature (green circle, mannose; yellow circle, galactose; blue square, GlcNAc; yellow square, GalNAc; red triangle, fucose). (For interpretation of the references to color in this figure legend, the reader is referred to the web version of this article.)

Table 2
Summary of lectin binding (+++ >50 intensity; ++ 30–50 intensity; + 10–30 intensity)*.

	Female			Male			
Lectin	Intestinal cytoplasm	Intestinal microvilli	Ovaries	Intestinal cytoplasm	Intestinal microvilli	Cement gland	Outer cuticle
Con A	+++	+++		+++	+++	+++	+
WGA		+++	+++		+++	+++	
SBA			+++				
UEA-I	++						

*Intensity means fluorescence intensity from lectin-stained images, as quantified using the ImageJ program.

peptides. We identified 380 sites located on 257 proteins using PNGase F-deglycosylated peptide mixtures (Table S2), and 109 sites present on 96 proteins using PNGase A-released peptide samples (Table S3). Most N-glycosylated sites (316 sites) could be entirely released by the PNGase F enzyme. Only 45 N-glycosylated sites were unique to the PNGase A-deglycosylated sample (Fig. 5A, Table S4), indicating the occurrence of α1,3-fucose in asparagine-linked GlcNAc residues. After attaching the shared subset (64 sites), a total of 425 N-glycosylated sites on 291 unique proteins composing the N-glycoproteome data were identified with high confidence (Fig. 5A, Table S4).

The number of N-glycosylated sites assigned on each protein ranged from 1 to 7 (average degree of glycosylation, 1.5). More than half of glycoproteins (210/291, 72%) carried only a single N-glycosylation site, 51 (18%) of them harbored double N-glycosylation sites, and the rest 30 (10%) contained three or more sites (Fig. 5B). The neighborhood residues of glycosylated asparagines may help determine the specificity of *H. contortus* oligosaccharyltransferase (OST), which transfers the dolichol-linked oligosaccharide precursor to the nascent polypeptides. The characteristic sequences of modified sites and their enrichment statistics were obtained by MoMo [27]. As shown in Fig. 5C, three conserved amino acids flanking the glycosylated asparagine residues (from −10 to + 10) were defined. These motifs included (N-x-T-*-Y), (N-x-T), and (N-x-S), where × represents any amino acid except for proline, and the *asterisk* denotes a random amino acid. Based on the hierarchical cluster analysis (Fig. 5D), threonine and serine displayed the highest probability at the position + 2, while the frequency of a proline residue in the proximity was markedly underrepresented. Therefore, the N-glycosylation sites in *H. contortus* matched with the canonical motif (N-x-T/S, x ≠ proline) while resonating with an earlier study on the free-living nematode *Caenorhabditis elegans* [28].

We tested the secondary structure and surface accessibility of glycosylated and non-glycosylated asparagines using the NetSrufP algorithm [22]. The analysis found that N-glycosylation was less likely to occur on the alpha-helix, as judged by a high probability of non-glycosylated asparagine (p = 1.39e^{-5}). In contrast, N-glycosylated residues were more likely to be positioned on the beta-strand (p = 0.0477) and disordered coil (p = 7.06e^{-6}) (Fig. 5E,

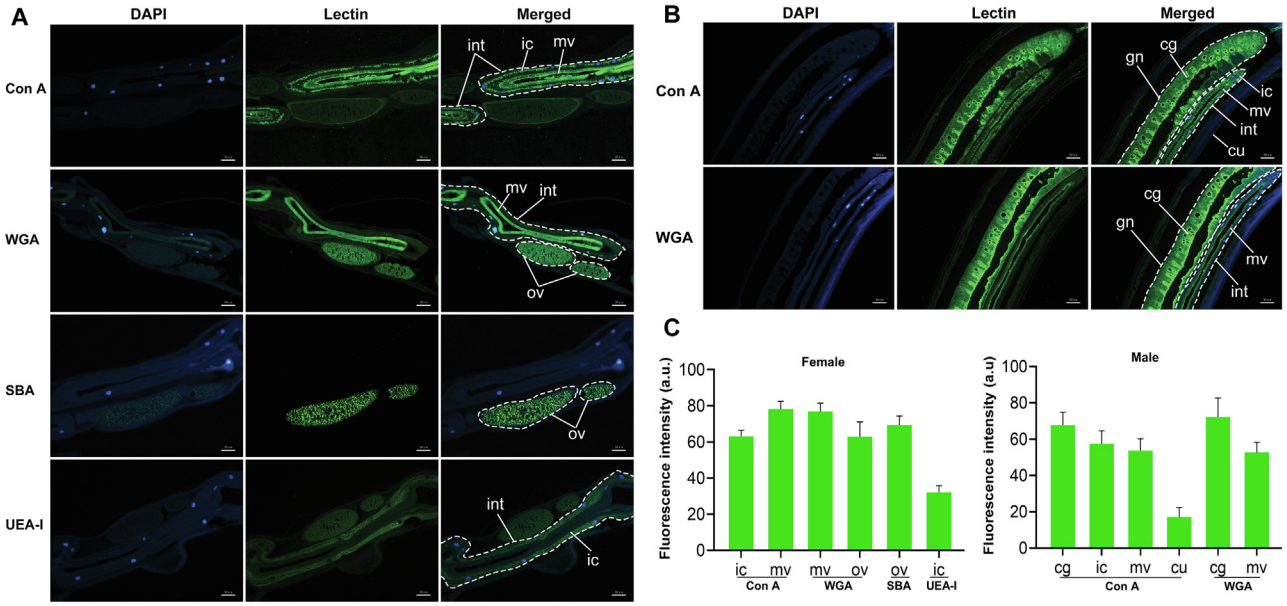

Fig. 4. Anatomical distribution of glycoconjugates in *Haemonchus contortus*. Paraffin-embedded sections of the adult female (A) and male (B) worms were probed with fluorescein-labeled lectins, as indicated (green). Nuclei were stained by DAPI (blue). Major tissues are outlined. Images shown here represent three independent assays. (C) The intensity of fluorescence signals from lectin-stained images in *panel A-B*. Graphs show the mean fluorescence intensity, as quantified using the ImageJ program (NIH, USA). Abbreviations: ic, intestinal cytoplasm; mv, microvilli; int, intestine; ov, ovaries; gn, male gonad; cg, cement gland; cu, cuticle (outer). Scale bars: 50 μm. (For interpretation of the references to color in this figure legend, the reader is referred to the web version of this article.)

left). As expected, the surface accessibility analysis suggested that the probability of modified asparagines on the protein surface was notably higher than non-N-glycosylated residues (p = 1.39e^{-7}) (Fig. 5E, *right*). These results, taken together, suggest a preference of the parasite OST for the beta-strand and coiled regions exposed to the surface of glycoproteins.

3.4. Functional analysis and predicted localization of glycosylated proteins

We finally examined the identified glycoproteins for predicted molecular function and subcellular localization to discern their physiological relevance (Fig. 6, Table S5-6). Notably, 23% and 13% of glycoproteins were associated with the binding function and hydrolase activity, respectively (Fig. 6A). Similarly, a sizeable fraction was predicted to localize in the extracellular space (51%), cytoplasm (15%), and plasma membrane (14%) (Fig. 6B). Other major glycoproteins supposedly reside in the endoplasmic reticulum (9%) and mitochondria (4%). The gene ontology (GO) enrichment (Table S7) demonstrated an association of identified glycoproteins with the terms 'extracellular matrix' and 'basement membrane' (Fig. 6C), further adding to the reliability of our N-glycoproteomic analysis, as the secreted proteins are often glycosylated. Among a total of 25 enriched protein domains, the cysteine protease family, laminin EGF-like domains, and peptidase family M1 were very abundant (Fig. 6D, Table S8). In particular, we identified cathepsin B-like cysteine proteinase (P25793), cysteine protease (A0A6F7NMZ2), and aminopeptidase (A0A140EQK0), which have two or more glycosylation sites and contain a potential α1,3-fucosylation on N^{99}, N^{197} and N^{745}, respectively (Fig. 6E).

4. Discussion

This study describing the N-glycome and N-glycoproteome of *H. contortus* complements the existing genomic, transcriptomic, and proteomic studies [29–32] and thereby fills a significant gap in our current understanding of this important parasitic nematode. The N-glycome of *H. contortus*, achieved by a fast atom bombardment mass spectrometer, was first reported well over two decades ago [17]. Compared to *state-of-the-art* technologies, the method had limited sensitivity and mass accuracy in detecting and classifying N-glycans. We deployed the MALDI-ToF-MS, which has become a method of choice for N-glycomics due to its high resolution, tolerance to impurities, and its ability to detect large complex glycans with high molecular weight [33]. Consequently, in conjunction with HILIC-LC-MS/MS, we identified a total of 425 N-glycosylated sites in 291 unique proteins in *H. contortus*. Our N-glycan data indeed obtained additional ion signals not reported in earlier FAB-MS analysis [17] that included Gal-Fuc-like modification and complex-type N-glycans appearing at m/z 1386.9, 1591.0, 1662.0, 1795.1, 2040.2, and 2255.4. Moreover, when compared to recent MALDI-MS data on PNGase A-released glycans [12], we observed glycans with a terminal GalNAc/GlcNAc at m/z 1662.0, 1795.1, 1836.1, 1907.1, 2040.2, 2214.3, and 2255.4 (Table S1), many of which may carry LDN or LDNF epitopes on antennae. Such differences are likely due to different amidase utilized for releasing glycans and detection instruments.

PNGase A enzyme can release PNGase F-resistant glycans modified with core α1,3-fucose, but it is limited in cleaving complex oligosaccharides [4,25]. We here combined PNGase F and PNGase A enzymes to fully release N-glycans from glycopeptides, providing a complete N-glycome profile for *H. contortus*. Several findings (Table S1), such as the presence of highly fucosylated glycans, pauci-mannosidic, and high mannose structures resonate with earlier studies [12,17]. Notably, *H. contortus* harbors a range of N-glycan modifications absent in mammalian glycans, especially the Gal-Fuc, LDNF motifs and α1,3-fucosylation. Such '*non-mammalian*' glycans are critical for the parasite invasion and counter-regulation of the host immune response [34]. Immunological studies have shown that the core α1,3-fucose and LDNF epitopes are recognized by IgG antibodies in sheep vaccinated with *H. contortus* excretory/secretory glycoproteins [13,14]. Besides, α1,3-fucose is a target of IgE during *H. contortus* infection [35].

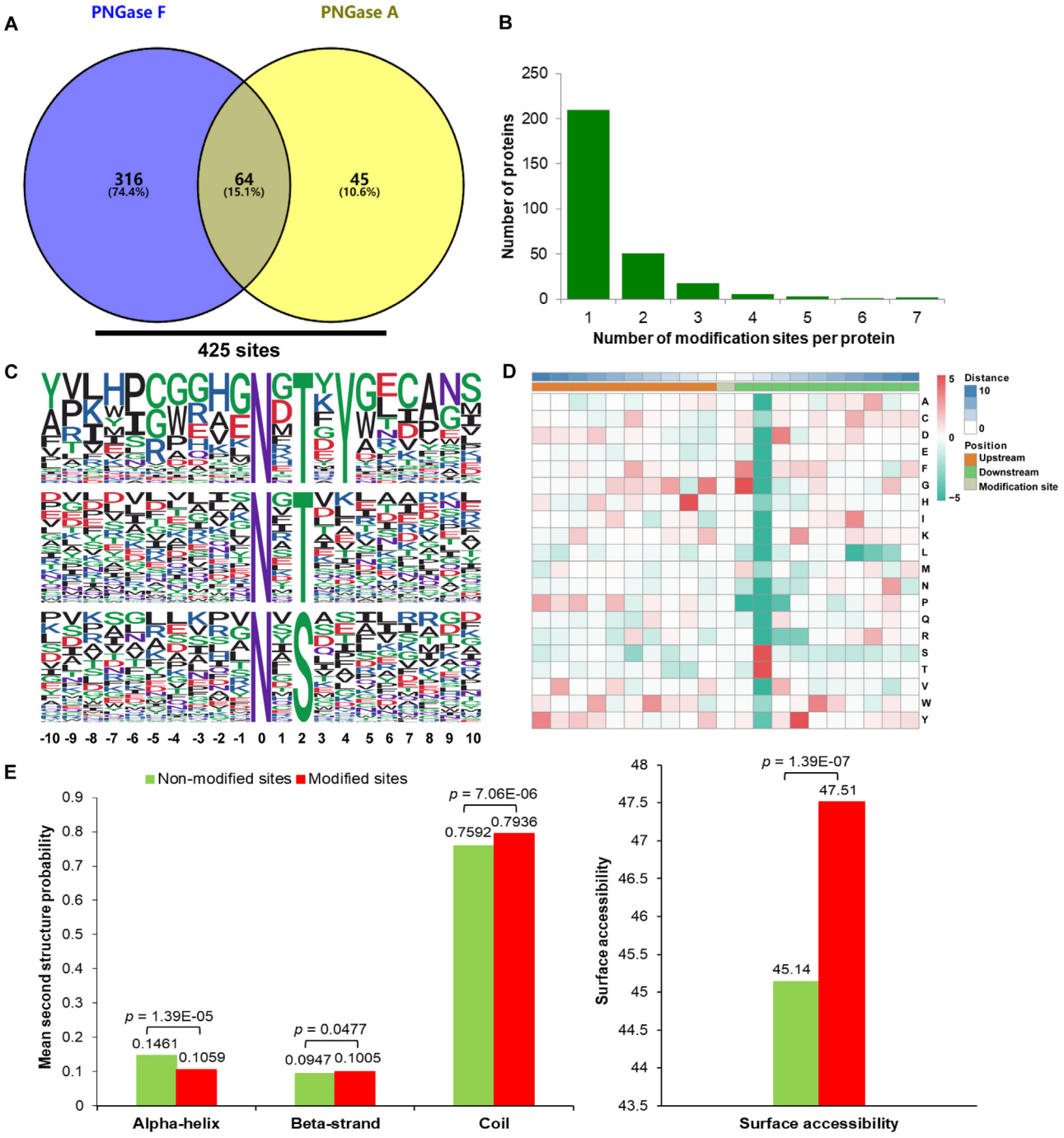

Fig. 5. Identification and topological features of N-glycosylated sites in *Haemonchus contortus*. (A) Venn diagram of the number of N-glycosylated sites released by PNGase F and PNGase A. (B) Distribution of N-glycosylated sites in detectable glycoproteins. (C) Sequence motifs located nearby the target asparagine in enriched glycosylation sites. (D) Heatmap showing the relative frequency of amino acids in the proximity of asparagine (enrichment, red; depletion, green). (E) Distribution of non-glycosylated and glycosylated asparagine residues in alpha-helix, beta-strand, and disordered coil (*left*), as well as the predicted surface topology of glycosylation sites (*right*). (For interpretation of the references to color in this figure legend, the reader is referred to the web version of this article.)

These glycan elements have also been reported in other parasitic helminths, *e.g.*, *Trichuris suis* and *Schistosoma mansoni* [36,37], and are being explored as novel targets for vaccines and diagnostics.

A majority of glycans are secreted and/or located on the parasite surface, forming a protective glycocalyx against the host defense systems [34]. Previous lectin-based localization data in the parasitic trematode *Fasciola hepatica* have shown that most glycoproteins are distributed on the spines, suckers and tegumental coat, which are continually replaced to escape the immune attack by the host [38]. We discovered that glycoconjugates in *H. contortus* are primarily *hidden* in the intestine and gonad, which may also impede their recognition by the host's immune system. Notably, initial works on *H. contortus* have suggested many immunogenic glycoproteins in the intestine (termed "*hidden* antigens") [39,40], *e.g.*, *H*11 and H-gal-GP, which may carry high mannose, LDNF and multiple fucose residues on N-glycans [17,41]. Staining with Con A, WGA and UEA-I lectins confirmed that glycoconjugates in

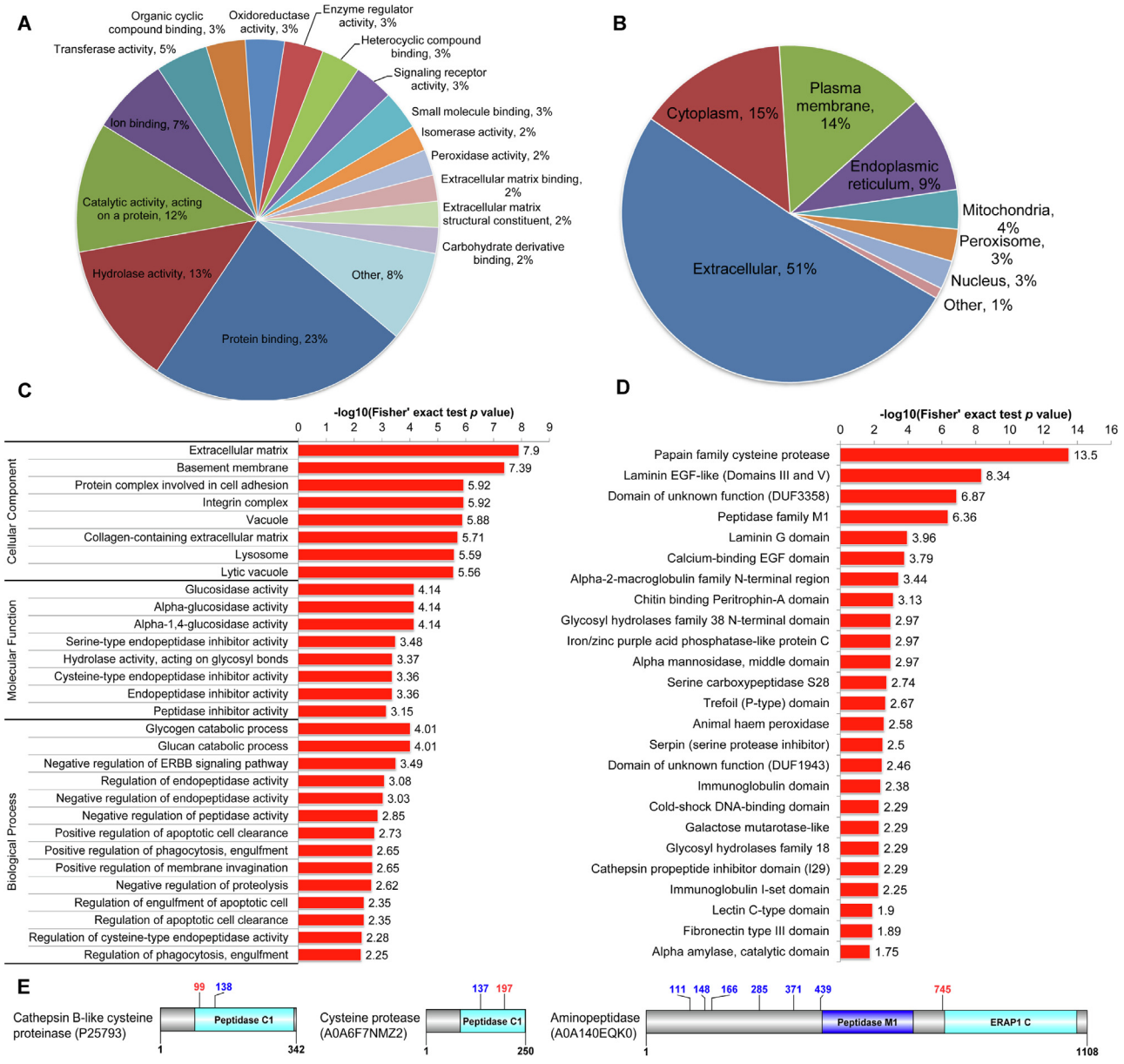

Fig. 6. Functional classification and enrichment analysis of *Haemonchus contortus* N-glycoproteins. (A-B) Classification of identified N-glycosylated proteins based on molecular function (A) and subcellular location (B), as indicated in *methods*. (C-D) Enrichment of N-glycoproteins based on gene ontology (C) and domain analyses (D). Numbers shown on the *x-axis* denote the statistical significance (values $\geq$ 1.3 indicate a *p*-value $\leq$ 0.05). (E) Predicted location of N-glycosylation sites in cathepsin B-like cysteine proteinase, cysteine protease and aminopeptidase. Numbers in red color represent the sites of α1,3-fucosylation on asparagine-linked GlcNAc residues, while the blue numerals show the glycosylation sites without α1,3-fucosylation on reducing terminal GlcNAc residues. (For interpretation of the references to color in this figure legend, the reader is referred to the web version of this article.)

the intestine are mostly glycosylated by mannose, GlcNAc and fucose-rich motifs. In brief, lectin-binding assays reveal the parasite intestine as a rich source of glycosylated antigens.

A vast majority of identified N-glycosylated sites matched the canonical motif (N-x-T/S, x ≠ proline), located primarily in the disordered coil regions on the protein surface, which echoes with the N-glycoproteome profiles of other model organisms, *C. elegans*, *Drosophila melanogaster* and *Danio rerio* [42]. We also predicted the secondary structure and surface accessibility of glycosylated and non-glycosylated motifs, revealing significant enrichment of the modified N-x-T in the alpha-helix regions (Fig S1). Several glycoproteins identified herein, *e.g.*, proteolytic peptidases, including peptidase C1 (cysteine peptidases, n = 32) and M1 (aminopeptidases, n = 8), were also found in a previous study of excretory/secretory proteins in *H. contortus* [43]. These molecules occur primarily in the intestine, facilitate hemoglobin degradation and nutrient acquisition, and are therefore expected to be essential for the growth, development and survival of hematophagous nematodes, *H. contortus*, *Ancylostoma caninum* and *Necator americanus* [44–46]. Due to critical physiological roles in parasitic worms, these peptidases are actively explored as prospective vaccine targets. Especially, the cysteine peptidases and aminopeptidases have been investigated widely in several immune protection trials against *H. contortus* [47].

The mutation of three predicted N-glycosylation sites on aminopeptidase was shown to significantly dampen the antibody response (about 95% reduction) compared with the native antigen [15], which suggested the antigenic importance of glycosylation sites. In this regard, we found that cathepsin B-like proteinase (P25793), cysteine protease (A0A6F7NMZ2) and aminopeptidase

(A0A140EQK0) harbor two or more glycosylated sites including a potential α1,3-fucosylated site. The α1,3-fucosylated glycoproteins of *C. elegans* are known to possibly induce Th2 type immune response in mice depending on the presence of intact glycans [48]. There are indeed N-glycosylation sites modified by glycans bearing *nematode-specific* motifs. The functional connectivity between unusual glycan structures and the specific glycosylation sites remains to be characterized by system-wide analysis of intact glycopeptide [7,49].

5. Conclusions

This study investigated the N-glycosylation profile of a parasitic nematode. Our glycopeptide enrichment-based mass spectrometry mapped the N-glycome and N-glycoproteome of *H. contortus*, disclosing several exclusive features. In extended work, we revealed the parasite intestine and gonad as the major sites of glycoconjugates' expression. Many glycoproteins with α1,3-fucosylation have been reported as potential vaccine candidates. Our work, therefore, lays the foundation to explore the biosynthesis and function of N-glycoproteins and thereby advance the therapeutic intervention against this widespread nematode parasite.

CRediT authorship contribution statement

Chunqun Wang: Methodology, Validation, Investigation, Data curation, Visualization, Writing - original draft. **Wenjie Gao:** Software, Formal analysis. **Shi Yan:** Formal analysis, Visualization. **Xing-Quan Zhu:** Resources. **Xun Suo:** Resources. **Xin Liu:** Software, Formal analysis. **Nishith Gupta:** Visualization. **Min Hu:** Conceptualization, Methodology, Validation, Visualization, Supervision.

Declaration of Competing Interest

The authors declare that they have no known competing financial interests or personal relationships that could have appeared to influence the work reported in this paper.

Acknowledgments

This study was supported by the National Natural Science Foundation of China (NSFC) (grant no. 31872462), the National Key Basic Research Program (973 program) of China (grant no. 2015CB150300) to Min Hu, and the Austrian Science Fund (grant no. P30021) to Shi Yan. Nishith Gupta acknowledges the financial support of the German Research Foundation (DFG) through a Heisenberg program grant (GU1100/16). The funders had no role in the study design, data collection and analysis, preparation, or decision to publish this work.

Appendix A. Supplementary data

Supplementary data to this article can be found online at https://doi.org/10.1016/j.csbj.2021.04.038.

References

[1] Alter G, Ottenhoff THM, Joosten SA. Antibody glycosylation in inflammation, disease and vaccination. Semin Immunol 2018;39:102–10.
[2] Dalziel M, Crispin M, Scanlan CN, Zitzmann N, Dwek RA. Emerging principles for the therapeutic exploitation of glycosylation. Science 2014;343 (6166):1235681. https://doi.org/10.1126/science.1235681.
[3] Engle DD, Tiriac H, Rivera KD, Pommier A, Whalen S, Oni TE, et al. The glycan CA19-9 promotes pancreatitis and pancreatic cancer in mice. Science 2019;364 (6446):1156–62.
[4] Shajahan A, Heiss C, Ishihara M, Azadi P. Glycomic and glycoproteomic analysis of glycoproteins-a tutorial. Anal Bioanal Chem 2017;409(19):4483–505.
[5] Poljak K, Selevsek N, Ngwa E, Grossmann J, Losfeld ME, Aebi M. Quantitative profiling of N-linked glycosylation machinery in yeast *Saccharomyces cerevisiae*. Mol Cell Proteomics 2018;17(1):18–30.
[6] Kailemia MJ, Xu G, Wong M, Li Q, Goonatilleke E, Leon F, et al. Recent advances in the mass spectrometry methods for glycomics and cancer. Anal Chem 2018;90(1):208–24.
[7] Ruhaak LR, Xu G, Li Q, Goonatilleke E, Lebrilla CB. Mass spectrometry approaches to glycomic and glycoproteomic analyses. Chem Rev 2018;118 (17):7886–930.
[8] Han D, Moon S, Kim Y, Min H, Kim Y. Characterization of the membrane proteome and N-glycoproteome in BV-2 mouse microglia by liquid chromatography-tandem mass spectrometry. BMC Genomics 2014;15(1):95. https://doi.org/10.1186/1471-2164-15-95.
[9] Jiang B, Huang J, Yu Z, Wu M, Liu M, Yao J, et al. A multi-parallel N-glycopeptide enrichment strategy for high-throughput and in-depth mapping of the N-glycoproteome in metastatic human hepatocellular carcinoma cell lines. Talanta 2019;199:254–61.
[10] Hoberg EP, Zarlenga DS. Evolution and biogeography of *Haemonchus contortus*: linking faunal dynamics in space and time. Adv Parasitol 2016;93:1–30.
[11] Yan F, Xu L, Liu L, Yan R, Song X, Li X. Immunoproteomic analysis of whole proteins from male and female adult *Haemonchus contortus*. Vet J 2010;185 (2):174–9.
[12] Paschinger K, Wilson IB. Two types of galactosylated fucose motifs are present on N-glycans of *Haemonchus contortus*. Glycobiology 2015;25:585–90.
[13] van Stijn CM, van den Broek M, Vervelde L, Alvarez RA, Cummings RD, Tefsen B, et al. Vaccination-induced IgG response to Galalpha1-3GalNAc glycan epitopes in lambs protected against *Haemonchus contortus* challenge infection. Int J Parasitol 2010;40:215–22.
[14] Vervelde L, Bakker N, Kooyman FNJ, Cornelissen AWCA, Bank CMC, Nyame AK, et al. Vaccination-induced protection of lambs against the parasitic nematode *Haemonchus contortus* correlates with high IgG antibody responses to the LDNF glycan antigen. Glycobiology 2003;13(11):795–804.
[15] Roberts B, Antonopoulos A, Haslam SM, Dicker AJ, McNeilly TN, Johnston SL, et al. Novel expression of *Haemonchus contortus* vaccine candidate aminopeptidase H11 using the free-living nematode *Caenorhabditis elegans*. Vet Res 2013;44(1):111. https://doi.org/10.1186/1297-9716-44-111.
[16] Munn EA, Smith TS, Grahama M, Greenwood CA, Tavernor AS, Coetzee G. Vaccination of merino lambs against haemonchosis with membrane-associated proteins from the adult parasite. Parasitology 1993;106(1):63–6.
[17] Haslam SM, Coles GC, Munn EA, Smith TS, Smith HF, Morris HR, et al. *Haemonchus contortus* glycoproteins contain N-linked oligosaccharides with novel highly fucosylated core structures. J Biol Chem 1996;271(48):30561–70.
[18] Liu X, Qiu H, Lee RK, Chen W, Li J. Methylamidation for sialoglycomics by MALDI-MS: a facile derivatization strategy for both alpha2,3- and alpha2,6-linked sialic acids. Anal Chem 2010;82:8300–6.
[19] Kang P, Mechref Y, Novotny MV. High-throughput solid-phase permethylation of glycans prior to mass spectrometry. Rapid Commun Mass Spectrom 2008;22(5):721–34.
[20] Jang-Lee J, Curwen RS, Ashton PD, Tissot B, Mathieson W, Panico M, et al. Glycomics analysis of *Schistosoma mansoni* egg and cercarial secretions. Mol Cell Proteomics 2007;6(9):1485–99.
[21] Kaji H, Saito H, Yamauchi Y, Shinkawa T, Taoka M, Hirabayashi J, et al. Lectin affinity capture, isotope-coded tagging and mass spectrometry to identify N-linked glycoproteins. Nat Biotechnol 2003;21(6):667–72.
[22] Meng X, Xing S, Perez LM, Peng X, Zhao Q, Redoña ED, et al. Proteome-wide analysis of lysine 2-hydroxyisobutyrylation in developing rice (*Oryza sativa*) seeds. Sci Rep 2017;7(1). https://doi.org/10.1038/s41598-017-17756-6.
[23] Yu NY, Wagner JR, Laird MR, Melli G, Rey S, Lo R, et al. PSORTb 3.0: improved protein subcellular localization prediction with refined localization subcategories and predictive capabilities for all prokaryotes. Bioinformatics 2010;26:1608–15.
[24] Jones P, Binns D, Chang H-Y, Fraser M, Li W, McAnulla C, et al. InterProScan 5: genome-scale protein function classification. Bioinformatics 2014;30 (9):1236–40.
[25] Yan S, Vanbeselaere J, Jin C, Blaukopf M, Wöls F, Wilson IBH, et al. Core richness of N-glycans of *Caenorhabditis elegans*: a case study on chemical and enzymatic release. Anal Chem 2018;90(1):928–35.
[26] Hokke CH, van Diepen A. Helminth glycomics - glycan repertoires and host-parasite interactions. Mol Biochem Parasitol 2017;215:47–57.
[27] Cheng A, Grant CE, Noble WS, Bailey TL. MoMo: discovery of statistically significant post-translational modification motifs. Bioinformatics 2019;35:2774–82.
[28] Kaji H, Kamiie J-I, Kawakami H, Kido K, Yamauchi Y, Shinkawa T, et al. Proteomics reveals N-linked glycoprotein diversity in *Caenorhabditis elegans* and suggests an atypical translocation mechanism for integral membrane proteins. Mol Cell Proteomics 2007;6(12):2100–9.
[29] Laing R, Kikuchi T, Martinelli A, Tsai IJ, Beech RN, Redman E, et al. The genome and transcriptome of *Haemonchus contortus*, a key model parasite for drug and vaccine discovery. Genome Biol 2013;14(8):R88. https://doi.org/10.1186/gb-2013-14-8-r88.
[30] Ma G, Wang T, Korhonen PK, Ang C-S, Williamson NA, Young ND, et al. Molecular alterations during larval development of *Haemonchus contortus* in vitro are under tight post-transcriptional control. Int J Parasitol 2018;48(9-10):763–72.

[31] Schwarz EM, Korhonen PK, Campbell BE, Young ND, Jex AR, Jabbar A, et al. The genome and developmental transcriptome of the strongylid nematode *Haemonchus contortus*. Genome Biol 2013;14(8):R89. https://doi.org/10.1186/gb-2013-14-8-r89.
[32] Wang T, Ma G, Ang C-S, Korhonen PK, Xu R, Nie S, et al. Somatic proteome of *Haemonchus contortus*. Int J Parasitol 2019;49(3-4):311–20.
[33] Shubhakar A, Kozak RP, Reiding KR, Royle L, Spencer DIR, Fernandes DL, et al. Automated high-throughput permethylation for glycosylation analysis of biologics using MALDI-TOF-MS. Anal Chem 2016;88(17):8562–9.
[34] Rodrigues JA, Acosta-Serrano A, Aebi M, Ferguson MAJ, Routier FH, Schiller I, et al. Parasite glycobiology: a bittersweet symphony. PLoS Pathog 2015;11(11):e1005169. https://doi.org/10.1371/journal.ppat.100516910.1371/journal.ppat.1005169.g00110.1371/journal.ppat.1005169.g002.
[35] van Die I, Gomord V, Kooyman FN, van den Berg TK, Cummings RD, Vervelde L. Core alpha1–>3-fucose is a common modification of N-glycans in parasitic helminths and constitutes an important epitope for IgE from *Haemonchus contortus* infected sheep. FEBS Lett 1999;463:189–93.
[36] Wilson IBH, Paschinger K. Sweet secrets of a therapeutic worm: mass-spectrometric N-glycomic analysis of *Trichuris suis*. Anal Bioanal Chem 2016;408(2):461–71.
[37] Smit CH, van Diepen A, Nguyen DL, Wuhrer M, Hoffmann KF, Deelder AM, et al. Glycomic analysis of life stages of the human parasite *Schistosoma mansoni* reveals developmental expression profiles of functional and antigenic glycan motifs. Mol Cell Proteomics 2015;14(7):1750–69.
[38] Ravidà A, Aldridge AM, Driessen NN, Heus FAH, Hokke CH, O'Neill SM, et al. *Fasciola hepatica* surface coat glycoproteins contain mannosylated and phosphorylated N-glycans and exhibit immune modulatory properties independent of the mannose receptor. PLoS Negl Trop Dis 2016;10(4):e0004601. https://doi.org/10.1371/journal.pntd.0004601.
[39] Smith WD, Newlands GFJ, Smith SK, Pettit D, Skuce PJ. Metalloendopeptidases from the intestinal brush border of *Haemonchus contortus* as protective antigens for sheep. Parasite Immunol 2003;25(6):313–23.
[40] Smith TS, Munn EA, Graham M, Tavernor AS, Greenwood CA. Purification and evaluation of the integral membrane protein H11 as a protective antigen against *Haemonchus contortus*. Int J Parasitol 1993;23:271–80.
[41] Geldhof P, Newlands GFJ, Nyame K, Cummings R, Smith WD, Knox DP. Presence of the LDNF glycan on the host-protective H-gal-GP fraction from *Haemonchus contortus*. Parasite Immunol 2005;27(1-2):55–60.
[42] Zielinska D, Gnad F, Schropp K, Wiśniewski J, Mann M. Mapping N-glycosylation sites across seven evolutionarily distant species reveals a divergent substrate proteome despite a common core machinery. Mol Cell 2012;46(4):542–8.
[43] Wang T, Ma G, Ang C-S, Korhonen PK, Koehler AV, Young ND, et al. High throughput LC-MS/MS-based proteomic analysis of excretory-secretory products from short-term in vitro culture of *Haemonchus contortus*. J Proteomics 2019;204:103375. https://doi.org/10.1016/j.jprot.2019.05.003.
[44] Williamson AL, Brindley PJ, Knox DP, Hotez PJ, Loukas A. Digestive proteases of blood-feeding nematodes. Trends Parasitol 2003;19(9):417–23.
[45] Jasmer DP, Rosa BA, Mitreva M, Dalton JP. Peptidases compartmentalized to the *Ascaris suum* intestinal lumen and apical intestinal membrane. PLoS Negl Trop Dis 2015;9(1):e3375. https://doi.org/10.1371/journal.pntd.0003375.
[46] Loukas A, Bethony J, Williamson A, Goud G, Mendez S, Zhan B, et al. Vaccination of dogs with a recombinant cysteine protease from the intestine of canine hookworms diminishes the fecundity and growth of worms. J Infect Dis 2004;189(10):1952–61.
[47] Newton SE, Meeusen ENT. Progress and new technologies for developing vaccines against gastrointestinal nematode parasites of sheep. Parasite Immunol 2003;25(5):283–96.
[48] Tawill S, Le Goff L, Ali F, Blaxter M, Allen JE. Both free-living and parasitic nematodes induce a characteristic Th2 response that is dependent on the presence of intact glycans. Infect Immun 2004;72(1):398–407.
[49] Suttapitugsakul S, Sun F, Wu R. Recent advances in glycoproteomic analysis by mass spectrometry. Anal Chem 2020;92(1):267–91.
[50] Ribeiro CV, Rocha BFB, Moreira DS, Peruhype-Magalhães V, Murta SMF. Mannosyltransferase (GPI-14) overexpression protects promastigote and amastigote forms of *Leishmania braziliensis* against trivalent antimony. Parasit Vectors 2019;12:60.
[51] Díaz MC, González NV, Zanuzzi CN, Najle R, Barbeito CG. Lectin histochemistry for detecting cadmium-induced changes in the glycosylation pattern of rat placenta. Biotech Histochem 2017;92(1):36–45.
[52] Hakami Z, Wakisaka S. Postnatal morphological and lectin histochemical observation of the submucosal glands of rat nasopharynx. Acta Histochem 2016;118(7):665–73.
[53] Labate M, Desantis S, Corriero A. Glycoconjugates during the annual sexual cycle in lizard epididymal ductuli efferentes: a histochemical study. Eur J Histochem 1997;41:47–56.